Superlubricity-activated thinning of graphite flakes compressed by passivated crystalline silicon substrates for graphene exfoliation

Amir Shakouri[a], Jingjie Yeo[b], Teng Yong Ng[a], Zishun Liu[c] and Hayden Taylor[a, d,*]

[a]School of Mechanical and Aerospace Engineering, Nanyang Technological University, 50 Nanyang Avenue, Singapore 639798

[b]A*STAR Institute of High Performance Computing, 1 Fusionopolis Way, Singapore 138632

[c] International Centre for Applied Mechanics, State Key Laboratory for Strength and Vibration of Mechanical Structures, Xi'an Jiaotong University, Xi'an, 710049, People's Republic of China

[d]Now with the Department of Mechanical Engineering, 6159 Etcheverry Hall, University of California, Berkeley 94720, USA

Abstract

A special thinning phenomenon is observed through molecular dynamics, where compression of AB-stacked graphite flakes between two hydrogen-terminated silicon substrates leads to the exfoliation of graphene layers. We have used multiple molecular dynamics simulations to study how this thinning phenomenon is affected by parameters such as size, number of graphene layers, and the crystalline orientation of the substrate surface. It is shown that this thinning phenomenon occurs through the activation of an inter-layer superlubricity regime, caused by torque-induced spontaneous rotations of the layers which is initiated by in-plane shear modes of graphite during compression.

1. Introduction

Graphene has been found to be a promising material for nanoelectronic devices on silicon-based substrates [1-2]. In order to produce graphene devices for research purposes, the "Scotch-tape" mechanical exfoliation method has been extensively used to produce single-layered graphene from highly ordered pyrolytic graphite (HOPG) [3]. These single layers can subsequently be transferred on to silicon/silicon dioxide substrates. Although the production of graphene using this method has been observed to achieve the highest electronic quality (e.g. mobility) to date [4], this production method is not readily scalable. Moreover, it suffers from possible contamination by glue residues as well as adsorbed water [5].

*Corresponding author. Tel: +1 510- 642-4901 Email: hkt@berkeley.edu (Hayden Taylor)

As such, research is on-going to obtain exfoliation of graphene on clean substrates [6-9] with no oxide layer using fusion bonding or direct wafer bonding [10]. However, these production methods have not been observed to be able to repeatedly attain large exfoliated areas of single-layer graphene. This limitation could be due to a lack of adhesion between these substrates and the graphene layers.

Since both the clean substrates and the graphene layers from HOPG flakes are crystalline, superlubricity behavior might be activated as another way of handling graphene layers on these substrates. In the superlubricity regime [11-13], friction systematically decreases between two crystalline surfaces in incommensurate contact. In addition to being crystalline, for a surface to be suitable for activating superlubricity, it must be atomically flat and hard, as superlubricity could break down if the contact surfaces are disordered, or if they undergo plastic deformations [14-15].

Moreover, in order to activate superlubricity between two surfaces, they should also be passivated, i.e. tend not to make covalent bonds [15]. Hydrogen-terminated (H-terminated) silicon substrates are examples of clean, crystalline, and passivated substrates which are quite stable, even at ambient conditions, due to fully co-ordinated surface atoms [16]. These clean substrates have been found to be suitable for activating superlubricity behavior [17].

On the other hand, it is also observed that the superlubricity regime can be activated in lamellar materials such as graphite [14] and molybdenum disulphide [18]. For these materials, superlubricity can usually be activated by rotating the layers with respect to each other. In particular, superlubricity behavior has recently been observed in HOPG, up to micrometer scales at ambient conditions [19-20]. Superlubricity behavior in carbon systems, such as multi-walled carbon nanotubes (MWCNTs), HOPG, and C60 molecules have been studied theoretically and experimentally [14, 21-23].

Spontaneous rotations have been observed when finite-sized graphite flakes slide on crystalline substrates (including graphite surfaces) in a superlubricity regime [22, 24]. It is shown in the present study, through molecular dynamics simulations, that a very similar phenomenon can be activated between the graphene layers in a finite-sized graphite flake when it is compressed by passivated crystalline substrates, leading to the thinning of the graphite flakes and exfoliation of single-layer graphene sheets. In this study, hydrogen-terminated silicon substrates are considered.

2. Simulation Methodology

The molecular dynamics (MD) simulation setup is as follows. The simulations are performed on the Large-scale Atomic/Molecular Massively Parallel Simulator (LAMMPS) [25] open source software. Periodic boundaries are prescribed in all directions to simulate bulk silicon substrate properties. The lateral dimensions of the simulation box are made sufficiently large to prevent interactions between the graphene layers in the neighboring periodic cell, even in a hypothetical situation where all graphene layers are exfoliated and aligned in one particular direction. Time integration is performed via the Velocity-Verlet method, using Nosé-Hoover style non-Hamiltonian equations of motion, generating positions and velocities sampled from the isothermal-isobaric (NPT) ensemble. The simulation occurs in a vacuum, thus mimicking dry contact between the substrates and the graphite flake. Initial velocities of atoms are randomly assigned as a Gaussian distribution, at an average temperature of 300 K.

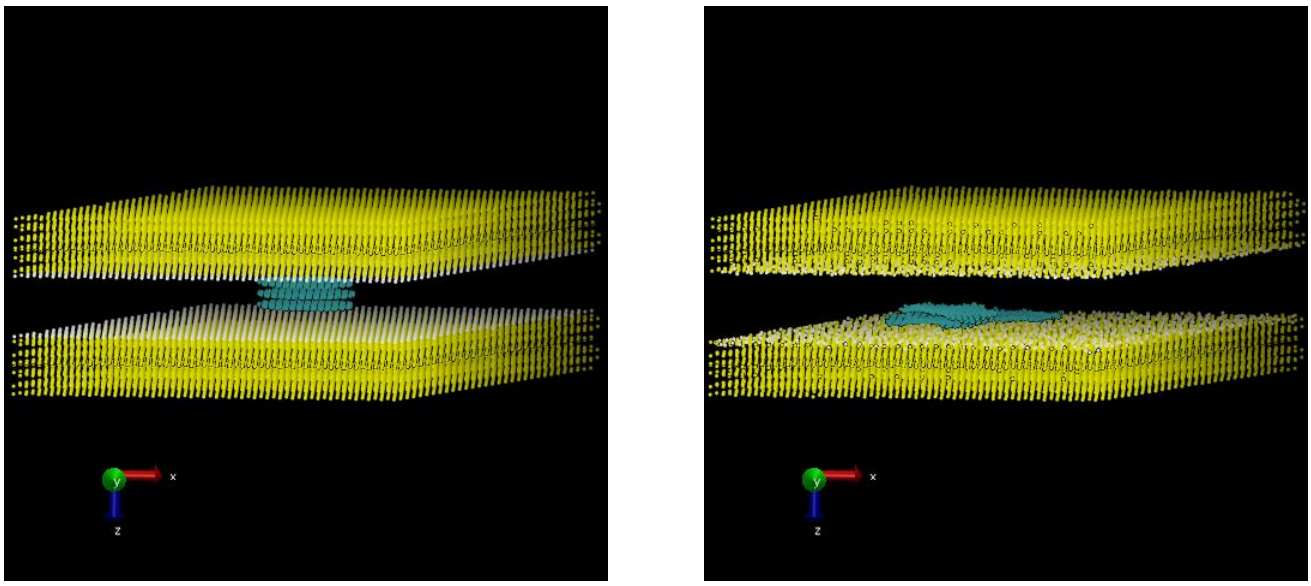

(a) (b)

Fig. 1 – (a) Initial and (b) final configurations of the molecular dynamics model for thinning of a tri-layer 3 nm graphite flake at 300 K using (111) H-terminated substrates. The graphene layers are exfoliated by applying the compression, and adhere to the substrate. Yellow, blue and white colours represent silicon, carbon and hydrogen atoms, respectively. Supplementary videos have also been provided on this MD simulation.

Fig. 1a illustrates an example of the molecular dynamics simulation setup. Finite-sized graphene layers stacked in AB form are considered to postulate the behavior of graphite flakes for this study. These flakes are also considered circular in shape. Finally, silicon substrates with specified crystalline surface orientations are considered in our study for compressing the graphite flake. The surfaces of these substrates are considered to be passivated by being terminated with hydrogen atoms, as shown in Fig. 1.

Interatomic interactions between carbon atoms are modeled using the Adaptive Intermolecular Reactive Bond Order (AIREBO) potential [26], implemented in LAMMPS as an extension of the second generation Reactive Bond Order (REBO) potential by Brenner [27]. This potential has been successfully and widely implemented in MD simulations to study the thermal and mechanical properties of carbon-based systems, including graphene [28-33]. The AIREBO potential consists of potential energies from the REBO potential, an intra-molecular interaction described by a "12-6" Lennard-Jones potential, and a bond torsional potential.

The AIREBO potential is capable of modelling covalent bond breakage and formation in carbon atoms, using empirically-fitted parameters in this classical mechanical potential, even though such changes are inherently quantum mechanical in nature. It allows for formation and dissociation of bonds during the MD run. Terms accounting for many-body interactions help to account for the local coordination environment of each atom, thus augmenting the conventional pairwise interactions. More crucially, this potential is able to describe the intra-molecular interactions between graphene layers, allowing us to accurately model the exfoliation phenomenon experienced during the compression of graphite flakes.

Intermolecular interactions between silicon and hydrogen atoms are modeled using the Tersoff potential [34-35], parameterized for Si-Si, Si-H and H-H bonds [36]. It has been shown that the Tersoff potential is able to reproduce accurately the elastic constants of pure silicon [37]. The C_{11}, C_{12} and C_{44} constants were found to be 150, 80 and 70 GPa respectively, in good agreement with experimental results [38].

Since the substrate is passivated, the interactions between the substrate and graphene layers are considered to be van der Waals only. The "12-6" Lennard-Jones potential is applied to simulate the interactions between carbon and silicon, as well as carbon and hydrogen. Eq. (1) expresses the Lennard-Jones potential, V in terms of the inter-atomic distance, r .

$$V(r) = 4\varepsilon\left[\left(\frac{\sigma}{r}\right)^{12} - \left(\frac{\sigma}{r}\right)^{6}\right] \quad (1)$$

The Lennard-Jones parameters, σ and ε, are determined using the Lorentz-Berthelot mixing rules [39], as stated in the Eq. (2) for interacting atoms 1 and 2. Using the Lennard-Jones parameters [26, 40] for carbon, silicon, and hydrogen, the Lennard-Jones parameters for any two atoms of differing elements have been obtained to be: $\sigma_{\text{C-Si}}$ = 0.280 nm, $\varepsilon_{\text{C-Si}}$ = 8.0109×10^{-22} J and $\sigma_{\text{C-H}}$ = 0.303 nm, $\varepsilon_{\text{C-H}}$ = 3.3005×10^{-22} J.

$$\sigma_{12} = \sigma_{21} = \frac{\sigma_1 + \sigma_2}{2}$$
$$\varepsilon_{12} = \varepsilon_{21} = \sqrt{\varepsilon_1 \varepsilon_2} \quad (2)$$

A time step of 0.5 fs is used. To begin the simulation, the entire system is equilibrated to the specified temperature over 25 ps. During the equilibration, the linear momentum of the graphite flake's centre of mass is nulled every 0.5 ps, preventing the graphite flake from drifting due to random fluctuations.

Thereafter, the graphite flake is slowly compressed by the silicon substrates. This compression is achieved by deforming the simulation box. This is done by moving the top boundary downwards along the z-axis at a constant rate of displacement of 2×10^{-6} nm/timestep, while the bottom boundary is fixed. This implies that the depth of the box is slowly decreasing, but the periodic boundary condition in the z-direction is not violated by this. Readers can refer to the video in the supplementary materials for an illustration of this deformation. Slower rates of displacements have also been checked to ensure that results are independent of the rate of displacement even though the process has been considered to be dynamic. The barostat in the out-of-plane direction was decoupled from all atoms during loading and unloading, ensuring that the calculated compressive stresses do not suffer from artifacts due to barostatting. The lateral directions are still coupled to the barostat, allowing for lateral relaxation to zero pressure throughout the entire loading and unloading process. Slower rates of displacements have also been checked to ensure that results are independent of the rate of displacement. The unloading rates are chosen to be double those of the loading rates to reduce the computational expense; we have determined that the exfoliation phenomenon is independent of the rate of unloading. The initial distance between the surfaces of the substrates and the graphite flake is considered to be 0.65 nm. The minimum distance achieved between the surfaces of the top and bottom substrate in each compression is 0.4 nm, which is close to the interlayer distance in graphite or the theoretical thickness of a single

layer of graphene. This approach ensures that sufficient compressive stress is achieved in the graphite flake during each compression.

The average compressive stress is determined by the summation of the stress in the z-direction of each atom in the graphite flake, divided by the total volume of the graphite flake[1]. The volume of each layer of the graphite flake is determined as the volume of a cylinder, where the diameter is given by the diameter of the flake. The height is the equilibrium interlayer distance of graphite, given [41] as 0.335 nm. The average stress in the silicon substrates is calculated similarly by the summation of the values of the stress per atom and divided by the volume of the silicon substrates in the unit cell.

3. Results & Discussion

Fig. 1 shows the initial and final configurations in a simulation where tri-layer graphite is compressed between H-terminated silicon plates. The mechanism of thinning in this simulation can be explained using the molecular dynamics outputs plotted in Fig. 2.

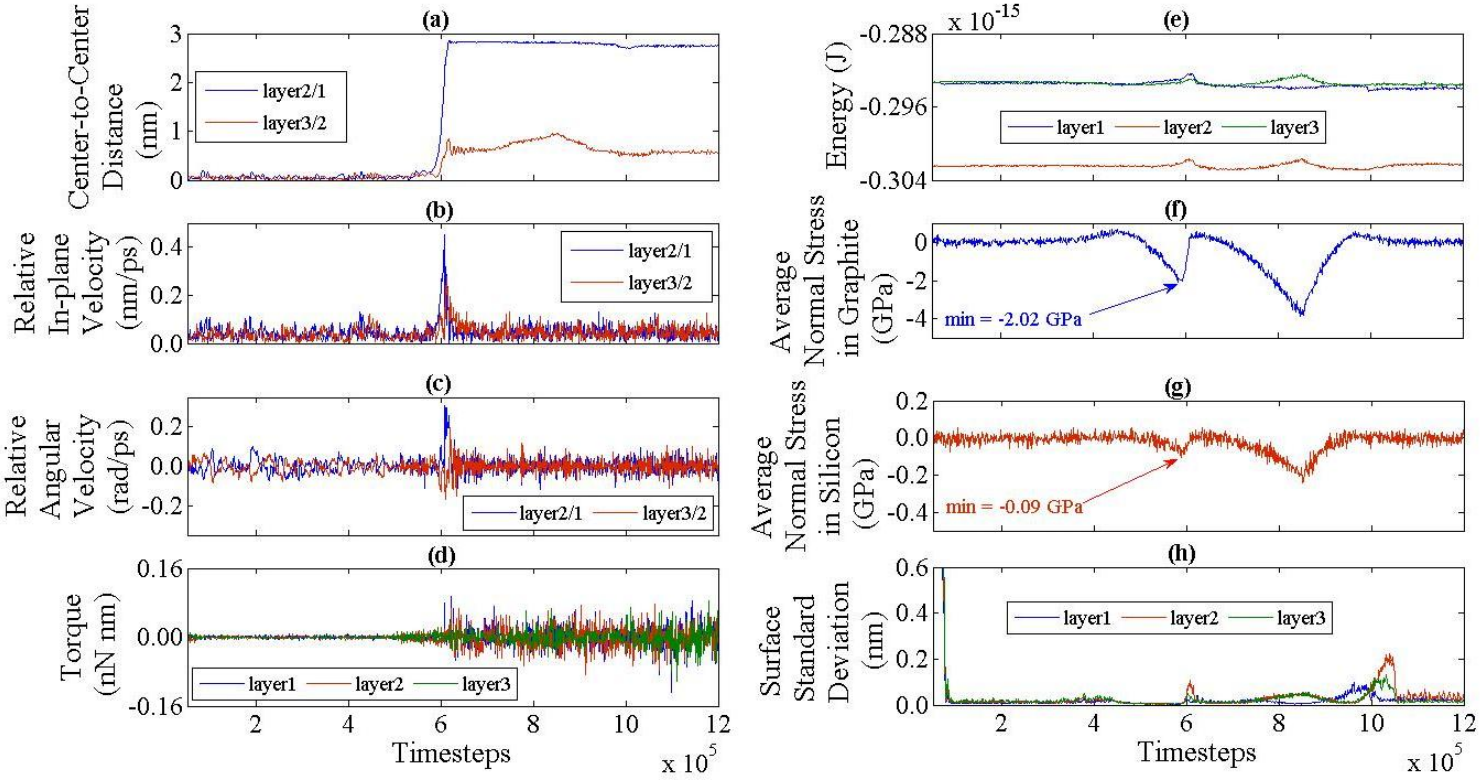

Fig. 2 – Molecular dynamics outputs calculated during compression of the 3 nm-diameter tri-layer graphite flake using H-terminated (111) silicon substrates. The symbol "/" stands for relative motions of the layers.

[1] http://lammps.sandia.gov/doc/compute_stress_atom.html

With reference to the initial configuration shown in Fig. 2a, the labels for plotting the data of each layer in Fig. 2 are as follows: the top, middle and the bottom layers have been considered as layers 1, 2 and 3, respectively. Fig. 2a shows the difference in magnitude of the lateral displacement between the centers of mass of the adjacent layers. The circular shape of the layers allows us to easily observe the exfoliation phenomenon through this plot. The thinning in this case consists of two exfoliations occurring almost at the same point of time around the 600,000th timestep. Fig. 2a shows that one of the exfoliations is almost complete while the other one is only partial.

Fig. 2b and Fig. 2c show the changes in the relative inter-layer in-plane velocities and the relative inter-layer angular velocities respectively. These results have been calculated using the velocities of the centers of mass of the individual layers and their angular velocities. As observed in Fig. 2b, an initial infinitesimal sliding motion exists between the layers which can be attributed to the atomistic thermal vibrations. Upon exfoliation, the magnitudes of the inter-layer in-plane velocities suddenly increase. The velocities will decrease again once the flake has fully exfoliated and relative motion is prevented due to flakes adhering to each other along the edges. This is illustrated in the videos provided as the supplementary materials. These changes in the inter-layer velocities are accompanied by sudden changes in the inter-layer angular velocities, demonstrating that during exfoliation, the layers not only slide with respect to each other but also rotate. Fig. 2d shows the total torque applied on each layer. For each layer of atoms in turn, we consider the contribution of every atom in that layer and calculate both the angular velocity and torque acting about the layer's centre of mass. As observed, during compression and particularly upon exfoliation of the layers, the magnitudes of the torques applied on the layers increase. This finding can explain the rotating motion of the layers with respect to each other.

Fig. 2e shows the changes in the total potential energy of the carbon atoms in each layer. The gap between the energy levels of layer 2 and those of layers 1 and 3 is due to the AB structure of the layers in the finite-sized graphite flake. Fig. 2f and Fig. 2g shows the average compressive stress experienced by the graphene layers and the silicon substrate, respectively.

Fig. 2e shows an initial drop in energies of the layers, between approximately 0 and 500,000 timesteps, which can be attributed to the adhesion of the graphite flake to the substrates prior to the compression. Subsequently, as the compression comes into effect and increases, strain energy is stored in the layers, and the energies of the layers increase. Subsequently, during exfoliation, some of the stored energies in the layers are released, and the layers reach to a new minimum state of energy. With

reference to Fig. 2b and Fig. 2c, it appears that these amounts of energies are converted to the kinetic energies required for the layers to slide and rotate.

During exfoliation, compressive stresses drop due to thinning. However, as observed in Fig. 2f and Fig. 2g, after the two-stage thinning in this case, further compression does not lead to further exfoliation in the layers. The maximum average compressive stress required to initiate the thinning and exfoliation, as experienced by the graphite flake and the silicon substrates, have been observed to be 2.02 GPa and 0.09 GPa, respectively. The latter can be assumed to be equal to the theoretical average external load required to initiate this thinning phenomenon.

Fig. 2h shows the standard deviation of the z-coordinate positions of the atoms in each of the graphene layers as a measurement of the layers' flatness during the compression. It is observed that prior to the occurrence of any exfoliation, the layers involved in the exfoliation are brought into highly flat configurations. Keeping this information in mind, and by considering the fact that inter-layer rotations are involved as observed in Fig. 2c, it can be concluded that the observed thinning phenomenon and the exfoliation of the layers are initiated by activating the superlubricity regime between the layers.

However, during exfoliation, the standard deviations of the out-of-plane deflections of the layers increase (Fig. 2e). These out-of-plane deformations serve as topographical roughness which tends to stop the superlubricity regime. As such, the thinning may not lead to a total exfoliation of the layers, as observed in Fig. 2a, particularly for the second stage exfoliation.

In order to better understand the superlubricity mechanism involved in the thinning of graphite flakes under compression using hydrogen-terminated silicon substrates, the effects of different parameters in the molecular dynamics simulations were studied. The parameters studied were the size (diameter) of the graphite flakes, number of the graphene layers in the flake, and the crystalline orientation of the substrate surfaces. Table 1 summarizes the values of the parameters considered for the different sets of studies.

Table 1 – Parameter sets considered for studies of the factors affecting compressive exfoliation.

Case Study Number	1	2	3	4	5	6
Number of Layers	2	2	2	3	3	2
Flake size (nm)	3	3	2	3	4	4
Substrate	(111)	(110)	(111)	(111)	(111)	(111)

For each of the six sets of conditions, four molecular dynamics simulations were run, assigning slightly different initial conditions for the velocity distributions of the atoms in each run. Totally, 24 simulations were conducted.

In reporting the results of the compression of the graphite flakes, for any two adjacent layers, we consider an increase of the center-to-center distance to at least 70 percent of the layers' diameter as a "major" exfoliation. Any increase which is less than 10 percent is not considered as exfoliation. Other cases are considered as "partial" exfoliation.

In the majority of simulations carried out, i.e. 19 out of 24, at least one major exfoliation is observed. For the tri-layer cases studied, partial exfoliations are also observed in addition to a major exfoliation. In all of these cases, it is observed that the graphite flakes are thinned and single graphene layers have been exfoliated as a result of compression.

In cases 1 to 5, exfoliation behavior is observed to occur frequently. In each of these cases, major exfoliations are observed in at least three of the four repetitions of the simulation. In Fig. 3, the maximum average compressive stress in the graphene flake that is required to initiate the thinning is compared across the five cases.

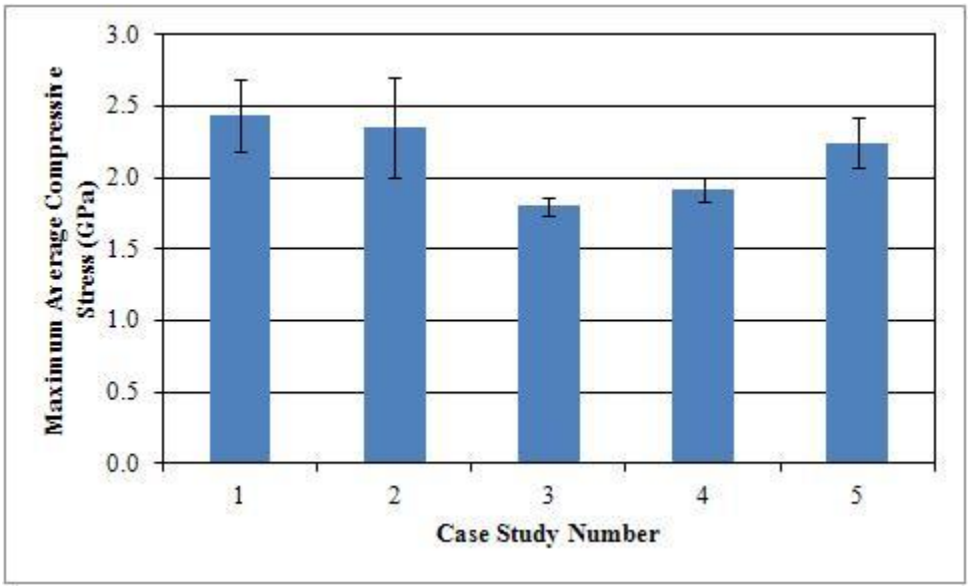

Fig. 3 – The maximum average compressive stress required by the graphite layers for activating thinning under five of the different sets of conditions specified in Table 1. Error bars show ±1 standard deviation of the maximum average compressive stress over replicate simulations.

A comparison between the compressive stresses observed in simulation cases 1 and 2 reveals insignificant difference. In these two sets of studies, bi-layer graphite disks of the same size are compressed using substrates with different crystalline surfaces. It can be established that the effect of the crystalline orientation of the substrates surfaces by itself is not significant in initiating the superlubricity behavior which results in thinning and exfoliation of the graphene layers. Instead, for studying the mechanism of thinning, the possible effect of the commensurate AB structure of the graphene layers, which is constant in these two sets of studies, should be explored.

Previous studies of the spontaneous rotation of sliding graphite flakes on crystalline substrates [22, 24] could help to explain the thinning phenomenon that is observed here. It was reported by Filippov et al. that the sliding and rotation of moving finite-sized graphite flakes on crystalline substrates (including a graphite surface itself) are coupled due to anisotropic friction [22]. Due to this coupling, as a result of sliding motions of the graphite flake on crystalline substrates, torque loads are applied on the flakes in addition to the friction, making them undergo spontaneous rotations. With these rotations, the graphite flakes tend to reorient from one potentially favorable state to another while sliding on the crystalline substrates.

The AB crystalline structure of graphite possesses in-plane lower shear thermal modes [42]. In these modes, the graphene layers perform in-plane vibration with respect to each other. Fig. 2c confirms the existence of such modes since, even prior to the thinning, the magnitude of the in-plane velocities of the layers relative to each other is not zero on average. Thus an infinitesimal sliding motion exists between the layers.

Due to the infinitesimal inter-layer sliding motions, a very similar phenomenon to that reported by Filippov et al. [22] can be stated to occur during the compression of the finite-sized graphite flake in our study. By applying compression, interlayer friction appears due to the atomistic surface energy corrugation of the layers. With the appearance of these inter-layer frictions, the shear modes of the layers are affected and the inter-layer sliding motion of the layers becomes coupled with inter-layer rotations. As a result of these interlayer rotations, the superlubricity regime is activated and the inter-layer frictions significantly decrease. This allows the graphene layers to move almost freely and become exfoliated. It should be noted that no shearing is externally applied for this thinning phenomenon to happen.

As discussed above, during exfoliation, out-of-plane deformations may also appear in the layers, tending to take the layers out of the superlubricity regime and hence stopping the thinning. In the majority of the cases studied, however, the thinning phenomenon has been observed to dominate, and these out-of-plane deformations do not fully prevent the exfoliation resulting in partial exfoliations in addition to at least one major exfoliation per case studied, as stated.

On the other hand, in extreme cases, when the graphite flakes are sufficiently large and thin, as in case 6 in Table 1, the out-of-plane deformations prevent any exfoliation from occurring at all i.e. the exfoliations observed are not more than 10 percent. Fig. 4 shows outputs from one such case.

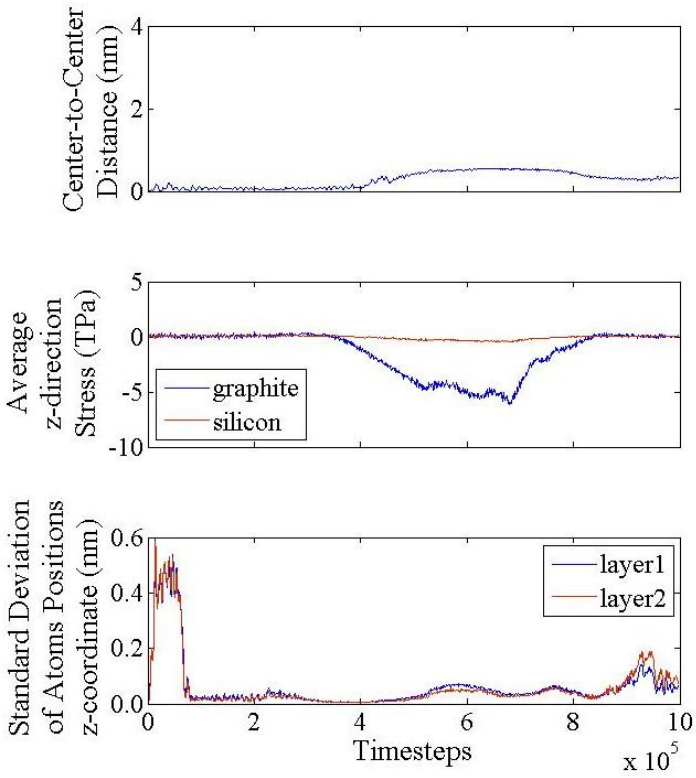

Fig. 4 – Molecular dynamics outputs calculated during compression of a non-exfoliating case of bi-layer 4 nm graphite flake using (111) H-terminated substrates.

It can be seen from Fig. 4a that thinning has not occurred, even though the compressive stress applied to the graphene layers, shown in Fig. 4b, is much larger than in the other cases studied, in which thinning is observed (Fig. 3). It is observed in Fig. 4c that in this case, the out-of-plane deformations

which appear at the start of thinning persist, stopping the superlubricity regime and preventing exfoliation.

From Fig. 3, it is generally observed that as the size of the graphene layers decreases or as the number of layers increases, the compressive stress required for initiating the thinning decreases. This can be observed by comparing the stresses corresponding to cases 1 and 3, 1 and 4, as well as 4 and 5, with each other.

It is observed that out-of-plane deformations of the layers are significant in preventing the thinning phenomenon for the extreme case of bi-layer 4 nm graphite flake studied in Fig. 4. By comparing how dominant the out-of-plane deformations of the layers are expected to be during the thinning of the graphite flakes reported in Fig. 3, the difference between the values of the average compressive stresses required for initiating the thinning can also possibly be explained. It is expected that when the graphite flakes become more "thin", i.e., when the number of the layers decreases or when the diameter of the flakes increases, the out-of-plane deformations of the layers become more dominant.

Hence, larger compression should be applied to suppress these out-of-plane deformations and to bring the layers to the flat configuration required for initiating the superlubricity regime. On the other hand, when the graphite flakes become less "thin", i.e. when the number of the layers increases or when the diameter of the flakes decreases, the out-of-plane deformations of the layers become less dominant and can be suppressed with less compression.

Finally, it is worth comparing the outcomes of compressing the flakes in cases 5 and 6. For sufficiently large 4 nm-diameter flakes, thinning is not observed to occur for the bi-layer cases, while it is observed to occur for the tri-layer cases. This result implies that for any size, if the graphite flakes are sufficiently thick, the thinning is expected to happen. This becomes important considering that the superlubricity behavior in the graphite layers – which has been shown here to be necessary for the thinning phenomenon to happen – was experimentally observed at ambient conditions for graphite flakes up to micrometer edge sizes [19] which are made from HOPG. As such, the studied thinning phenomenon may be applied for exfoliating graphene sheets from graphite flakes with sizes which are relevant for device manufacturing. All these suggest further experimental studies on compression of graphite flakes using passivated crystalline substrates. This type of process may open new routes in producing graphene on clean passivated substrates.

4. Conclusion

A thinning phenomenon of graphite flakes as a result of compression using hydrogen-terminated silicon substrates was reported and studied via molecular dynamics simulations. As a result of this thinning behavior, major and partial exfoliations of graphene layers were observed. It was shown that this phenomenon is initiated by activating an inter-layer superlubricity regime. The superlubricity regime was shown to be activated by spontaneous rotations which occur as a result of coupling between the inter-layer rotations and sliding due to shear thermal modes in the graphite flakes during compression. The dependence of thinning behavior on flake size, number of graphene layers, and crystalline orientation of the substrates was studied by comparing the compressive stress required for thinning to initiate. Out-of-plane deformations of the layers during thinning tend to halt the superlubricity regime that is required for exfoliation to occur but the thinning behavior is observed to be dominant when the graphite flakes are sufficiently thick. Further experimental studies may lead to a new approach of graphene production on clean passivated substrates.

Acknowledgements

This research was supported by the Infocomm Development Authority of Singapore (IDA) Cloud Computing Grant #6 for cloud computing and storage resources. This work was also supported by the Agency for Science, Technology and Research (A*STAR), Republic of Singapore, and the A*STAR Computational Resource Centre. A. Shakouri and H. Taylor are grateful for support from an NTU faculty start-up grant. The authors would like to thank Professor Huajian Gao and his research group in Brown University, for their extremely helpful and useful comments on this work.

References

[1] Kim K, Choi JY, Kim T, Cho SH, Chung HJ. A role for graphene in silicon-based semiconductor devices. Nature. 2011;479(7373):338-44.

[2] Soldano C, Mahmood A, Dujardin E. Production, properties and potential of graphene. Carbon. 2010;48(8):2127-50.

[3] Novoselov KS, Jiang D, Schedin F, Booth TJ, Khotkevich VV, Morozov SV, et al. Two-dimensional atomic crystals. Proceedings of the National Academy of Sciences of the United States of America. 2005;102(30):10451-3.

[4] Bolotin KI, Sikes KJ, Jiang Z, Klima M, Fudenberg G, Hone J, et al. Ultrahigh electron mobility in suspended graphene. Solid State Communications. 2008;146(9-10):351-5.

[5] Lin YC, Lu CC, Yeh CH, Jin C, Suenaga K, Chiu PW. Graphene annealing: How clean can it be? Nano Letters. 2012;12(1):414-9.

[6] Akcöltekin S, El Kharrazi M, Köhler B, Lorke A, Schleberger M. Graphene on insulating crystalline substrates. Nanotechnology. 2009;20(15).
[7] Chen CC, Aykol M, Chang CC, Levi AFJ, Cronin SB. Graphene-silicon Schottky diodes. Nano Letters. 2011;11(5):1863-7.
[8] Ritter KA, Lyding JW. Characterization of nanometer-sized, mechanically exfoliated graphene on the H-passivated Si(100) surface using scanning tunneling microscopy. Nanotechnology. 2008;19(1).
[9] Ochedowski O, Begall G, Scheuschner N, El Kharrazi M, Maultzsch J, Schleberger M. Graphene on Si(111)7×7. Nanotechnology. 2012;23(40).
[10] Christiansen SH, Singh R, Gösele U. Wafer direct bonding: From advanced substrate engineering to future applications in micro/nanoelectronics. Proceedings of the IEEE. 2006 2006;94(12):2060-105.
[11] Hirano M, Shinjo K. Atomistic locking and friction. Physical Review B. 1990;41(17):11837-51.
[12] Hirano M, Shinjo K, Kaneko R, Murata Y. Anisotropy of frictional forces in muscovite mica. Physical Review Letters. 1991;67(19):2642-5.
[13] Hirano M, Shinjo K, Kaneko R, Murata Y. Observation of superlubricity by scanning tunneling microscopy. Physical Review Letters. 1997;78(8):1448-51.
[14] Dienwiebel M, Verhoeven GS, Pradeep N, Frenken JWM, Heimberg JA, Zandbergen HW. Superlubricity of graphite. Physical Review Letters. 2004;92(12):126101-1.
[15] Müser MH. Structural lubricity: Role of dimension and symmetry. Europhysics Letters. 2004;66(1):97-103.
[16] Kolíbal M, Čechal J, Bartošík M, Mach J, Šikola T. Stability of hydrogen-terminated vicinal Si(1 1 1) surface under ambient atmosphere. Applied Surface Science. 2010;256(11):3423-6.
[17] Masuda H, Honda F. Low friction of a diamond/H-terminated Si(111) sliding system. IEEE Transactions on Magnetics. 2003;39(2 I):903-8.
[18] Martin JM, Donnet C, Le Mogne T, Epicier T. Superlubricity of molybdenum disulphide. Physical Review B. 1993;48(14):10583-6.
[19] Liu Z, Yang J, Grey F, Liu JZ, Liu Y, Wang Y, et al. Observation of microscale superlubricity in graphite. Physical Review Letters. 2012;108(20).
[20] Zheng Q, Jiang B, Liu S, Weng Y, Lu L, Xue Q, et al. Self-retracting motion of graphite microflakes. Physical Review Letters. 2008;100(6).
[21] Dienwiebel M, Pradeep N, Verhoeven GS, Zandbergen HW, Frenken JWM. Model experiments of superlubricity of graphite. Surface Science. 2005;576(1-3):197-211.
[22] Filippov AE, Dienwiebel M, Frenken JWM, Klafter J, Urbakh M. Torque and twist against superlubricity. Physical Review Letters. 2008;100(4).
[23] Verhoeven GS, Dienwiebel M, Frenken JWM. Model calculations of superlubricity of graphite [91]. Physical Review B - Condensed Matter and Materials Physics. 2004;70(16):1-10.
[24] Depondt P, Ghazali A, Lévy JCS. Self-locking of a modulated single overlayer in a nanotribology simulation. Surface Science. 1998;419(1):29-37.
[25] Plimpton S. Fast Parallel Algorithms for Short-Range Molecular-Dynamics. J Comput Phys. 1995 Mar 1;117(1):1-19.
[26] Stuart SJ, Tutein AB, Harrison JA. A reactive potential for hydrocarbons with intermolecular interactions. J Chem Phys. 2000 Apr 8;112(14):6472-86.
[27] Brenner DW, Shenderova OA, Harrison JA, Stuart SJ, Ni B, Sinnott SB. A second-generation reactive empirical bond order (REBO) potential energy expression for hydrocarbons. J Phys-Condens Mat. 2002 Feb 4;14(4):783-802.

[28] Yeo JJ, Liu ZS, Ng TY. Comparing the effects of dispersed Stone-Thrower-Wales defects and double vacancies on the thermal conductivity of graphene nanoribbons. Nanotechnology. 2012;23(38).
[29] Ng TY, Yeo JJ, Liu ZS. A molecular dynamics study of the thermal conductivity of graphene nanoribbons containing dispersed Stone-Thrower-Wales defects. Carbon. 2012;50(13):4887-93.
[30] Shenoy VB, Reddy CD, Ramasubramaniam A, Zhang YW. Edge-stress-induced warping of graphene sheets and nanoribbons. Physical Review Letters. 2008;101(24).
[31] Zhao H, Min K, Aluru NR. Size and chirality dependent elastic properties of graphene nanoribbons under uniaxial tension. Nano Letters. 2009;9(8):3012-5.
[32] Xu L, Ma T-b, Hu Y-z, Wang H. Molecular dynamics simulation of the interlayer sliding behavior in few-layer graphene. Carbon. 2012;50(3):1025-32.
[33] Sandoz-Rosado EJ, Tertuliano OA, Terrell EJ. An atomistic study of the abrasive wear and failure of graphene sheets when used as a solid lubricant and a comparison to diamond-like-carbon coatings. Carbon. 2012;50(11):4078-84.
[34] Tersoff J. Modeling solid-state chemistry: Interatomic potentials for multicomponent systems. Phys Rev B. 1989;39(8):5566-8.
[35] Tersoff J. Erratum: Modeling solid-state chemistry: Interatomic potentials for multicomponent systems. Phys Rev B. 1990;41(5):3248-.
[36] De Brito Mota F, Justo JF, Fazzio A. Hydrogen role on the properties of amorphous silicon nitride. J Appl Phys. 1999;86(4):1843-7.
[37] Tersoff J. Empirical interatomic potential for silicon with improved elastic properties. Physical Review B. 1988;38(14):9902-5.
[38] Tersoff J. New empirical approach for the structure and energy of covalent systems. Physical Review B. 1988;37(12):6991-7000.
[39] Allen MPTDJ. Computer simulation of liquids. New York: Oxford University Press 1989.
[40] Zimmerman PM, Head-Gordon M, Bell AT. Selection and validation of charge and lennard-jones parameters for QM/MM simulations of hydrocarbon interactions with zeolites. Journal of Chemical Theory and Computation. 2011;7(6):1695-703.
[41] Delhaes P. Graphite and precursors: Australia ; [Great Britain] : Gordon & Breach, c2001. 2001.
[42] Tan PH, Han WP, Zhao WJ, Wu ZH, Chang K, Wang H, et al. The shear mode of multilayer graphene. Nature Materials. 2012;11(4):294-300.